Effect of the ordered interfacial water layer in protein complex formation: A nonlocal electrostatic approach

A. Rubinstein,[1,*,†] R. F. Sabirianov,[2,*,‡] W. N. Mei,[2] F. Namavar,[3] and A. Khoynezhad[1]
[1]*Department of Biomedical Sciences and Surgery, Creighton University Medical Center, Omaha, Nebraska 68131, USA*
[2]*Department of Physics, University of Nebraska at Omaha, Omaha, Nebraska 68182, USA*
[3]*Department of Orthopaedic Surgery and Rehabilitation, University of Nebraska Medical Center, Omaha, Nebraska 68198, USA*
(Received 22 April 2010; published 18 August 2010)

Using a nonlocal electrostatic approach that incorporates the short-range structure of the contacting media, we evaluated the electrostatic contribution to the energy of the complex formation of two model proteins. In this study, we have demonstrated that the existence of an ordered interfacial water layer at the protein-solvent interface reduces the charging energy of the proteins in the aqueous solvent, and consequently increases the electrostatic contribution to the protein binding (change in free energy upon the complex formation of two proteins). This is in contrast with the finding of the continuum electrostatic model, which suggests that electrostatic interactions are not strong enough to compensate for the unfavorable desolvation effects.

DOI: 10.1103/PhysRevE.82.021915 PACS number(s): 87.15.km, 87.15.kr

I. INTRODUCTION

Adequate and accurate calculations of the intramolecular and intermolecular electrostatic interactions (EI) in a polar solvent are very important for the analysis of structural, as well as functional features of bimolecular and colloidal nanoparticles in medical, biological and bioengineering applications. These interactions contributing to the formation of protein complexes, oligomers, and/or other complex structures are actively studied [1–4]. The recent progress in nanobiotechnology indicates that a more detailed understanding of intramolecular EI at the molecular scale is needed [5–10]. Furthermore, the knowledge of these interactions is necessary for sufficient description of the protein adsorption mechanisms on nanostructured implant surfaces, as well as in studies of the interfacial protein-protein interactions that determine biocompatibility of the various implant surfaces in bioengineering applications.

The analysis of many protein associations has shown that the opposite charged and polar residues located in the vicinity of binding sites tend to form interprotein electrostatic contacts [1,11–17]. It was found, both experimentally and theoretically, that the favorable EI between the two associating proteins could be an essential factor for this binding process [1,2,11–15,17–30]. Specifically, according to the aforementioned theoretical works [1,13,17,26,27], the existence of favorable electrostatic binding thoroughly explains the experimentally measured rate constants for protein association. However, several theoretical works promote an alternate opinion [31–34]. The calculations of the Coulomb interactions in these works, performed in the framework of the continuum classical electrostatic model [35–37], suggest that these interactions are generally not strong enough to compensate for the unfavorable desolvation effects. Thus, it is still uncertain whether the EI favor the process of protein binding.

The electrostatic free energy (ΔG_{EI}) of binding two interacting macromolecules, in particular proteins A and B into the complex AB, in an aqueous solvent can be computed as the difference in the electrostatic free energy between bound (ΔG^{AB}) and unbound ($\Delta G^{\mathrm{A}}+\Delta G^{\mathrm{B}}$) protein states [1]:

$$\Delta G_{\mathrm{EI}} = \Delta G^{\mathrm{AB}} - (\Delta G^{\mathrm{A}} + \Delta G^{\mathrm{B}}) = \frac{1}{2}\left[\sum_{i\in(\mathrm{A,B})} (q_i\Phi_i)^{\mathrm{AB}} - \sum_{i\in\mathrm{A}} (q_i\Phi_i)^{\mathrm{A}} - \sum_{i\in\mathrm{B}} (q_i\Phi_i)^{\mathrm{B}}\right], \quad (1)$$

where the summation is over all the charges q_i located in the macromolecule(s), and Φ_i is the electrostatic potential at the position of q_i. Ordinarily, the electrostatic potential is calculated using the Poisson-Boltzmann equation in the framework of classical electrostatics with a local relation between the field and its electric induction [1,35,38].

In view of the present uncertain opinions regarding the essential role of EI on molecular binding in an aqueous solution, it is necessary to point out that both groups of the theoretical works, mentioned above, were treating the interfacial water molecular layer as bulk, i.e., assuming that its dielectric constant to be ~80. It should be noted that this model, however, may be incorrect even in a general case. Many experimental [39–41] and theoretical works based on molecular dynamic simulations [42–46] (see also [38] and references cited therein) suggest that the solvent near the protein surface forms an effective layer of partially structured interfacial water with dielectric properties distinct from the bulk solvent.

Recently, in the framework of a continuum nonlocal (NL) electrostatic model adopting an integral relationship between the electric field and its induction, it was shown that including the dynamic solvent microstructure stipulates the spatial heterogeneity of the effective dielectric properties of both protein and solvent at their interface [38,47]. In particular, the rather extended water shell occurs at the protein-solvent interface with substantially reduced dielectric permittivity. This effect results in the prominent decline of the electric

*Corresponding author.
†arubinstein@mail.unomaha.edu
‡rsabirianov@mail.unomaha.edu

field screening in vicinity to the interface. It was also shown that the high magnitude of the rate constants in the association protein kinetics can be explained by the existence of the extended low-dielectric interfacial water shells, mentioned above, through which EI between two protein subunits are accomplished [47].

In our study, to assess the role in the electrostatic contribution to the binding free energy of protein-protein association (ΔG_{EI}), we considered a simple system that is composed of two model macromolecular particles, in particular proteins A and B. Single point charges of opposite signs are located at their respective surfaces in the region of functional patches (binding sites). The bound state of the complex AB assumes the contact of these particles at the location of opposite charges by their binding sites. To estimate EI energy of the point charge placed into the isolated particle (A or B) in close proximity to the solvent interface (ΔG^{A}, ΔG^{B}) we calculated the corresponding "charge image potential" (IP) acting on the above charge due to its electrostatic interaction with the induced polarization at the interface [48–51]. We adopted the concept of the NL electrostatics and phenomenological theory of polar solvent [38,47] (and references cited therein). Assuming that the charges located at the protein binding sites are in close proximity to their molecular surface, the interface in the vicinity of the charge was approximated as a locally flat (planar) solvated region.

Based on our asymptotic and numerical analysis of the IP potential, we conclude that the charge placed in the protein (solute) near the solvent interface experiences relatively moderate attraction to the interface in comparison with the significantly larger attraction calculated in the classical solvent models. As a result, in this case the electrostatic contribution of the protein binding free energy is much stronger and can be consider an important factor to compensate for the unfavorable desolvation effects in the formation of the protein complex.

II. METHODS

In the present work, we applied the NL electrostatic approach to calculate the electrostatic interactions at the model protein-solvent interface [38,47]. In this approach, the linear dielectric response for each of the media in contact is presented by the integral nonlocal relation between the electric induction **D** and the electric field **E**:

$$D_{\mathrm{m},\alpha}(\mathbf{r}) = \sum_{\beta} \int_{Vm} \varepsilon_{\mathrm{m},\alpha\beta}(\mathbf{r},\mathbf{r}') E_{\mathrm{m},\beta}(\mathbf{r}') d\mathbf{r}', \quad \alpha,\beta = x,y,z, \tag{2}$$

where $m=1$, 2 refers to the media, solvent and solute; the function $\varepsilon_{\mathrm{m},\alpha\beta}(\mathbf{r},\mathbf{r}')$ is the dielectric permittivity tensor that is determined by the spatial correlation induced by the polarization of the medium; and the integration is taken over the volume V_m of the medium. The main purpose of this approach is to incorporate the short-range structure of the contacting media into electrostatics.

For simplicity, we adopted the planar dielectric boundary that models the local regions of the interface between proteinlike medium (solute) and solvent (i.e., both media are semi-infinite). The cylindrical coordinate system, (R,Z), was introduced for this boundary, where Z is the axis perpendicular to the plane passing through the boundary, and R is the two-dimensional radius vector in this plane (Fig. 1). As shown in Fig. 1, the semi-infinite regions $Z<0$ and $Z>0$ were assigned to a solvent and a solute, respectively. The charge $Q=\xi_e$ (ξ is the fraction of the electron charge e) is located in the solute at point $(0, Z_0)$.

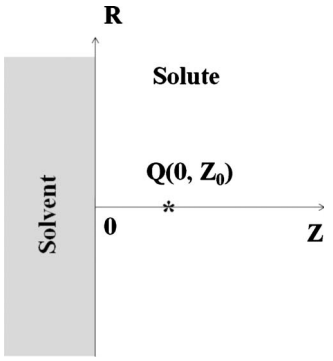

FIG. 1. The charge Qlocated at the point $(0, Z_0)$ of the cylindrical coordinate system, Z_0 is the distance to the interface.

In the framework of the so-called "specular reflection approximation" model for the system of two semi-infinite media [38,47,48,50], which we adopted here, the properties of the media along the plane of the boundary are considered as homogeneous isotropic with $\varepsilon_{\mathrm{m},\alpha\beta}(\mathbf{r},\mathbf{r}') = \varepsilon_{\mathrm{m},\alpha\beta}(Z,Z',\mathbf{R}\text{-}\mathbf{R}')$ and can be expressed through the bulk dielectric function [48]. In order to compute the electrostatic potential $\varphi(R,Z,Z_0)$ created by charge Q in any point (R,Z) with $Z>0$, we combined the first Maxwell's equation, i.e., Gauss's Law, with non-local relationship Eq. (2). This allows one to express the potential in terms of the Fourier-transformed dielectric functions $\varepsilon_1(\mathbf{r}\text{-}\mathbf{r}')$ and $\varepsilon_2(\mathbf{r}\text{-}\mathbf{r}')$ [$\varepsilon_1(k)$ and $\varepsilon_2(k)$, respectively], which characterize the bulk dielectric properties of the solvent and solute, respectively [38,48,49]:

$$\varphi(R,Z,Z_0) = \frac{1}{2\pi}\int_0^{+\infty} dK K J_0(KR)\varphi(K,Z,Z_0), Z_0, Z > 0 \tag{3}$$

where:

$$\varphi(K,Z,Z_0) = 4Q\int_{-\infty}^{\infty} dK_z \frac{e^{\mathrm{i}K_z Z}}{k^2\varepsilon_2(k)}\left\{\cos(K_z Z_0) - \frac{\mathrm{A}(K)}{\mathrm{B}(K)}\right\}$$

$$\mathrm{A}(K) = \int_{-\infty}^{\infty} dK_z \frac{\cos(K_z Z_0)}{k^2\varepsilon_2(k)},$$

$$\mathrm{B}(K) = \int_{-\infty}^{\infty} \frac{dK_z}{k^2}\left\{\frac{1}{\varepsilon_1(k)} + \frac{1}{\varepsilon_2(k)}\right\},$$

$$k^2 = K^2 + K_z^2, \tag{4}$$

$$K^2 = \sum_{\alpha=x,y} K_\alpha^2,$$

$$\varepsilon_m(k) = \sum_{\alpha,\beta} (K_\alpha K_\beta / K^2) \int_{Vm} d(r\text{-}r') \exp[-ik(r\text{-}r')] \varepsilon_{m,\alpha\beta}(r\text{-}r'),$$

and J_0 (KR) is the Bessel function of the first kind.

The derived potential allows for the calculation of the IP potential $W(Z_0)$, which is a change in free energy of the system when transferring charge Q from infinity (bulk of the solute) to the point $R=0$, $Z=Z_0$ at the interface. This energy is determined by the Güntelberg charging cycle using the Fourier-Bessel transformation [50,51]:

$$W(Z_0) = \frac{Q}{4\pi} \lim_{Z \to Z_0} \int_0^{+\infty} dK K[\varphi(K,Z,Z_0) - \varphi^0(K,Z,Z_0)] \quad (5)$$

where $\varphi(K,Z,Z_0)$ is given by Eq. (4), and $\varphi^0(K,Z,Z_0)$ denotes the electrostatic potential when the charge located at infinity and can be obtained by setting $Z, Z_0 \to +\infty$ in Eq. (4):

$$\varphi^0(K,Z,Z_0) = 2Q \int_{-\infty}^{\infty} dK_z \frac{e^{iK_z(Z-Z_0)}}{k^2 \varepsilon_2(k)}. \quad (6)$$

In order to analyze the behavior of the IP potential, the solute was considered as a uniform dielectric with low dielectric constant $\varepsilon_2(k)=\varepsilon_p=4$, taking into account small dipolar fluctuations in proteins [52]. The dielectric function $\varepsilon_1(k)$ in the bulk of the aqueous solvent in Eq. (4) was approximated in the context of polar solvent phenomenological model [38,47,50]:

$$\varepsilon_1(k) = \varepsilon* + (\varepsilon_s - \varepsilon*)/[1 + (Lk)^2 \varepsilon_s/\varepsilon*], \quad (7)$$

where $\varepsilon*=6$ and $\varepsilon_s=78.3$ are short- and long-wavelength dielectric constants of the solvent at room temperature; and L is the correlation length of the water dipoles, which is proportional to the characteristic length of the hydrogen-bonding network of water molecules (~3–5 Å). The dielectric function $\varepsilon_1(k)$ is the "one pole approximation" that considers the orientational Debye polarization (caused by the rotations of water dipoles, which, in turn, are hindered by the hydrogen-bonding chains) and neglects the higher frequency (infrared, electronic or optical) modes [38,53–55]. This simple model suggests that in liquid water the whole spectrum of the polarization fluctuations can be divided into two zones: (i) the low-frequency zone associated with the orientational Debye mode; and (ii) the high-frequency zone associated with infrared and optical modes. Due to the strong nonelectrostatic interactions, the polarizations within the orientational mode are correlated (with some effective correlation radius L) in space, while the polarizations within the high-frequency modes are assumed to be noncorrelated [53,56]. The dielectric constant, determined within the transparency zone of the electromagnetic absorption (which separates frequencies typical for low- and high-frequency zones), corresponds to the short-wavelength dielectric constant $\varepsilon*$ [53,56]. Thus, the "one pole approximation" dielectric model for liquid water assumes that the function $\varepsilon_1(k)$ is changed at the length-scale $\sim L$ from the values characteristic for the macroscopic, long-wavelength dielectric constant, ε_s, to the value of the short-wavelength dielectric constant $\varepsilon \cong 6$ [53,54,56]. It should be mentioned that the "one pole approximation" is appropriate for the description of polar molecules without internal degrees of freedom, such as rigid, strong correlated dipoles [53].

It is very important to note that the quantities $\varepsilon*$ and L in the bulk dielectric permittivity of liquid water provide good fits to the experimental data analyzed in terms of the free energy of interaction between protonated amino groups in dibasic amines [55]. It should be noted also that $\varepsilon_1(k)$ function, Eq. (7), is an insightful solvent dielectric model that was applied in the framework of the NL electrostatic approach to explain several experimental data in the electrolyte theory, interfacial electrochemistry, and computational biophysics (see [38,47] and references cited therein).

III. RESULTS AND DISCUSSION

In order to estimate the electrostatic free energy of binding of two proteins forming the complex we considered a model of two idealized (spherical) proteins A and B of similar size. Each protein possesses a single ion charge of opposite sign located at the protein surface interacting patches or protein "binding sites." We considered each ion as a point charge located in the solute, at the proximity of its molecular surface. This approach is similar to the one proposed by Rubinstein and Sherman [47] for estimation of protein association rate in solvent.

The bound state AB occurs through the contact of the corresponding binding sites (facing each other) of proteins A and B. We asserted that the opposite point charges ($Q_A=\xi e$ and $Q_B=-\xi e$, $\xi=1$) belonging to the binding sites form the ion pair with minimal inter-charge distance r_{12}. This distance is about $r_{12}=2r_{ion} \approx 5$ Å, where $r_{ion} \approx 2.5$ Å is the maximum proximity of a charged center of an ionogenic group of amino acid residue to the molecular protein surface. The radius of the globular protein R_p is usually much larger than r_{ion} ($r_{ion}/R_p \ll 1$), for example, in the case of globular proteins and their complexes, as well as biological and artificial (nonorganic) supramolecular structures. Consequently, the interface in the vicinity of the charge can be considered as planar to estimate the electrostatic component of the free energy of binding in the bound state. However, when R_p is comparable with r_{ion} (i.e., a curvature of the interface cannot be neglected), the corresponding correction needs to be included.

In the case of planar interface, the electrostatic free energy of the bound system described by the first term of Eq. (1) is Coulomb interaction energy in a proteinlike medium (AB complex) with the dielectric constant $\varepsilon_P=4$ and the intercharge distance r_{12} mentioned above:

$$\Delta G^{AB} = Q_A Q_B/(\varepsilon_p r_{12}) = -28 \ k_B T, \quad (8)$$

where $k_B T$ is Boltzmann's constant times the absolute temperature of the system ($k_B T \approx 0.593$ kcal/mol at 25 °C).

To estimate the electrostatic free energy of the proteins in the unbound states ΔG^A and ΔG^B we calculated the IP potential, Eq. (5), that is equivalent to the change of electrostatic free energy of one protein when the charge Q (Q_A or

Q_B) is transferred from infinity (the bulk of the solute) to the point $R=0$, $Z=Z_0$ at the interface (Fig. 1).

Omitting cumbersome computations, the $W(Z_0)$ potential in the k_BT energy units can be written in the form of (see Appendix):

$$W(Z_0)/(560\ k_BT\xi^2) = (4\varepsilon_p Z_0)^{-1}\int_0^{+\infty} dxS(x,\eta)\exp(-x),$$

$$S(x,\eta) = [D(x,\eta) - 1/\varepsilon_p]/[D(x,\eta) + 1/\varepsilon_p],$$

$$D(x,\eta) = (1/\varepsilon_S) + (1/\varepsilon* - 1/\varepsilon_S)[1 + (x\eta)^{-2}]^{-1/2}, \quad (9)$$

where $\eta=L/2Z_0$ is a dimensionless parameter, and $Q^2 = \xi^2 e^2 = 560\ k_BT\xi^2$.

The IP potential, Eq. (9), calculated in the framework of the NL electrostatic approach, is reduced to the classical expression $W_{cl}(Z_0)$ of two uniform dielectrics when $\varepsilon_s=\varepsilon*$ (or $L=0$) [37]:

$$\frac{W_{cl}(Z_0)}{560\xi^2 k_BT} = \frac{1}{4Z_0\varepsilon_p}\frac{\varepsilon_p - \varepsilon_S}{\varepsilon_p + \varepsilon_S}. \quad (10)$$

To analyze the dependence of the IP potential, Eq. (9), on the distance Z_0 from the interface, we carried out both the asymptotic and numerical analysis.

The asymptotic expansion of the integral Eq. (9) was performed for the limiting large and small values of $L/2Z_0$. Although in some cases these asymptotic limits are outside of the physical scales, yet they still reveal features of the $W(Z_0)$ function that can be compared with classical results. Simple estimations of $W(Z_0)$ were carried out by taking the first terms of the expansions. The following asymptotic expression is:

$$\frac{W(Z_0)}{560\xi^2 k_BT} = \frac{1}{4Z_0\varepsilon_p}\begin{cases}(\varepsilon_p - \varepsilon_*)/(\varepsilon_p + \varepsilon_*), & Z_0 \ll L\\ (\varepsilon_p - \varepsilon_S)/(\varepsilon_p + \varepsilon_S), & Z_0 \gg L\end{cases}. \quad (11)$$

These asymptotic solutions are similar to those of the air-solvent interface obtained in the framework of the NL model when $\varepsilon_p=1$ [57]. As it follows from Eq. (11), there is a characteristic length, $Z_0 \sim L$, that divides the entire solvent space into two parts, i.e., $Z_0 < L$ and $Z_0 > L$, and shows the distinct behaviors of $W(Z_0)$. The asymptotic solution Eq. (11) for $Z_0 \gg L$ is equivalent to the classical function Eq. (10) determined for any $Z_0 > 0$, while the corresponding asymptotic solution Eq. (11) at the $Z_0 \ll L$ is significantly different from the classical solution. Thus, the IP potential [Eq. (9)] at the very small values $Z_0 \ll L$ asymptotically approaches the expression as if the dielectric constant of the solvent is $\varepsilon*$, while at the very large values $Z_0 \gg L$ the IP approaches the corresponding expression as if the dielectric constant of solvent is ε_S. All of these findings suggest that there is an effective reduction of the dielectric function of the solvent in close proximity to the interface when considering the IP potential at small enough Z_0. This effect is consistent with our results in the case of pairwise EI at the protein-solvent interface [38,47].

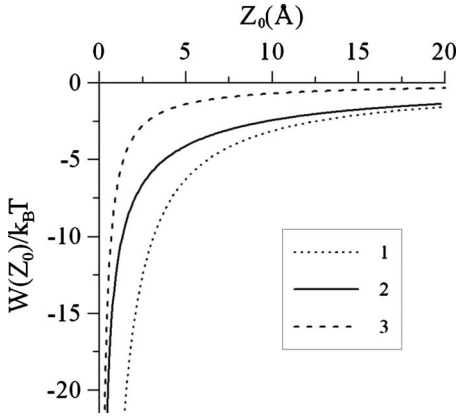

FIG. 2. The numerical calculation of $W(Z_0)$ as a function of the distance Z_0 to the interface. Parameters of the solvent for the curves 1–3: (1: dotted line) $\varepsilon_S=\varepsilon*=78.3$, $W_{cl}(Z_0=2.5\ \text{Å})=-12.6\ k_BT$; (2: solid line) $\varepsilon*=6$, $\varepsilon_s=78.3$, $L=5$ Å, $W(Z_0=2.5\ \text{Å})=-6.6\ k_BT$; (3: dashed line) $\varepsilon_S=\varepsilon*=6$, $W_{cl}(Z_0=2.5\ \text{Å})=-2.8\ k_BT$. For all cases the dielectric constant of the solute $\varepsilon_p=4$.

Numerical calculations of the $W(Z_0)$ and $W_{cl}(Z_0)$ functions were performed using Eqs. (9) and (10), respectively. Results of these calculations are shown in Fig. 2. In this figure we compare the behavior of the IP potential estimated by the NL model ($\varepsilon*=6$, $\varepsilon_s=78.3$, $L=5$ Å) and the classical local model ($\varepsilon*=\varepsilon_s=78.3$) of the aqueous solvent. As seen in Fig. 2, numerical calculations are consistent with our asymptotic analysis. At the very small distances $Z_0 \ll L = 5$ Å, the values of the IP potential $W(Z_0)$ approaches to the values of the classical function $W_{cl}(Z_0)$ calculated using short-wavelength dielectric constants of the solvent ($\varepsilon_s=\varepsilon*=6$). At the distances $Z_0 > L (Z_0 \approx 6-8$ Å) the IP potential Eq. (9) approaches the values of the classical function Eq. (10) with $\varepsilon_s=78.3$, and at the very large $Z_0 \gg L$ the curve 2 almost coincide with the asymptotic values that are equivalent to the classical case with $\varepsilon_2=\varepsilon*=78.3$ (curve 1).

The above asymptotic and numerical analysis, complemented with results of our recent works [38,47] (carried out in the framework of the NL electrostatic approach for the pairwise EI energy at the model protein-solvent interface), suggests that a layer of interfacial water on the protein surface has effective dielectric properties different from the bulk solvent. In fact, the effective dielectric permittivity of the solvent is a function of distance from the interface. The magnitude of the function is $\sim(\varepsilon_p+\varepsilon*)/2$ at small $Z \sim Z_0 < L$ (in close proximity to the interface), while it approaches $\sim(\varepsilon_p+\varepsilon_S)/2$ at the large distances $Z \sim Z_0 > 10-15$ Å. The validity of these average dielectric constants at the interface is also supported by recent work [58]. It should also be noted that the occurrence of a low-dielectric layer on the protein surface is consistent with the experimental study of hydration dynamics on the protein surface [41,47] (and references cited therein).

When considering IP at the distance $Z_0 < L$, the majority of the induced boundary charges at the interface is localized in the proximity of point charges Q_A or Q_B and decrease rapidly along the interface approximately as $\sim Z_0/(R^2 + Z_0^2)^{3/2}$ [37,58]. Thus, the planar interface approximation of-

fers an accurate estimation of the main electrostatic contribution to the change of the free energy of the unbound model protein due to charging. Hence, the electrostatic free energy of the unbound protein states ($\Delta G^A + \Delta G^B$) is determined by summing the two identical IP potentials calculated by Eq. (9).

Overall, the asymptotic and numerical analysis shows that, in close proximity to the solvent within region $Z_0 \sim L$ at the protein-solvent interface, the charge experiences relatively moderate effective favorable electrostatic binding to the interface in comparison with estimations based on the classical solvent models with the dielectric constant of the solvent ~80. In other words, the EI energy between the point charge in the solute and interface (or IP) is significantly less than the corresponding energy estimated using the classical approach. For example, the direct estimation of ΔG_{EI} for $Z_0 = r_{ion} \sim 2.5$ Å in the classical model using Eq. (9) ($\varepsilon_p = 4$, $\varepsilon_S = \varepsilon* = 78.3$) and data for $W_{cl}(Z_0)$ shown in Fig. 2 gives:

$$\Delta G_{EI} = \Delta G^{AB} - (\Delta G^A + \Delta G^B) = -28\ k_B T - 2(-12.6\ k_B T) = -2.8\ k_B T,$$

while numerical calculation carried out using NL approximation Eq. (9) ($\varepsilon_p = 4$, $\varepsilon* = 6$, $\varepsilon_s = 78.3$, $L = 5$ Å) (see Fig. 2) gives substantially larger value of ΔG_{EI}:

$$\Delta G_{EI} = \Delta G^{AB} - (\Delta G^A + \Delta G^B) = -28\ k_B T - 2(-6.6\ k_B T) = -15\ k_B T.$$

Therefore, we have shown that taking into account the reduced effective permittivity of the solvent on the interface strongly affects the electrostatic contribution to the binding energy of proteins. Using the simple idealized model system of the two interacted proteins, we have shown that the electrostatic free energy of binding (ΔG_{EI}) can be remarkably larger than that estimated by the classical approach. Thus, the analysis of protein binding should include the NL solvent effects together with the microstructure of the solvent surrounding proteins. Our results clearly suggest that the electrostatic component of the protein binding is an important factor to compensate for the unfavorable desolvation effects in the formation of the protein complex, contrary to the findings of the continuum classical electrostatic model for the aqueous solvent.

IV. CONCLUSIONS

We adopted a recently developed NL electrostatic approach, which was designed to evaluate the pairwise EI in protein at the protein-solvent interface [38], to estimate the electrostatic free energy of two proteinlike particles in unbound ($\Delta G^A + \Delta G^B$) states. These energies were considered as IP acting on the charges immersed in the proteinlike medium at the interface. The binding energy (ΔG_{EI}) is evaluated as the difference between the electrostatic free energy of the system in bound (ΔG^{AB}) and those in unbound ($\Delta G^A + \Delta G^B$) states.

Results of the present study suggest that the charge placed in a protein (solute) near the solvent interface experiences relatively moderate effective electrostatic binding to the interface in comparison to the significantly larger electrostatic binding estimated by the classical solvent models. Consequently, the electrostatic contribution to the protein binding is found to be significantly stronger than that estimated by the classical solvent model. We stress that this contribution is an important factor to compensate for the unfavorable desolvation effects in the formation of the protein complex.

Asymptotic and numerical analysis of the image potential points to the occurrence of the effective low-dielectric layer of water on the protein surface, which is consistent with our previous results [38,47]. It should be noted that the boundary water layer appears naturally in the framework of the NL approach, without consideration of the specific interactions of the water molecules with the protein surface.

Overall, our results vigorously suggest that the above interfacial solvent layer (the partially structured water layer on the protein surface), called "dynamically ordered water" [40], can be a major factor determining the possible compensation for the unfavorable desolvation effects in the formation of the protein complexes. Similar conclusions can be made about the desolvation effects during the formation of protein adhesion on the inorganic artificial (implant) surfaces where planar approximation used in the present study could be applied directly.

ACKNOWLEDGMENTS

We thank Dr. Tim Doerr (National Center for Biotechnology Information, NIH) and Dr. Simon Sherman (University Nebraska Medical Center, Omaha) for fruitful discussions. A.R. and A.K. work was supported by the Nebraska Tobacco Settlement Biomedical Research Development Award (Grant No. NE-LB-692); State of Nebraska, Department of Health and Human Services. R.F.S., W.N.M., and F.N. work was supported by Nebraska Research Initiative and NSF.

APPENDIX: CALCULATION OF IMAGE POTENTIAL

Using Eqs. (4) and (6), one can rewrite Eq. (5) for the IP potential $W(Z_0)$ in the form of:

$$W(Z_0) = (Q^2/2\pi)\int_{-\infty}^{+\infty} dK K\{g_1(K,Z_0) - 2[g_2(K,Z_0)g_3(K,Z_0)]/[g_3(K,Z_0=0) + g_4(K)]\}, \tag{A1}$$

where

$$g_1(K,Z_0) = \int_{-\infty}^{+\infty} dK_Z \exp(i2K_Z Z_0)/[k^2\varepsilon_2(k)],$$

$$g_2(K,Z_0) = \int_{-\infty}^{+\infty} dK_Z \cos(K_Z Z_0)/[k^2\varepsilon_2(k)],$$

$$g_3(K,Z_0) = \int_{-\infty}^{+\infty} dK_Z \exp(iK_Z Z_0)/[k^2\varepsilon_2(k)],$$

$$g_4(K) = \int_{-\infty}^{+\infty} dK_Z/[k^2\varepsilon_1(k)].$$

All integrals from $g_1(K,Z_0)$ to $g_4(K)$ in Eq. (A1) were calculated by the method of complex contour integration on the complex plane K_Z. The dielectric functions $\varepsilon_2(k)$ and $\varepsilon_1(k)$ inserted in corresponding integral expressions in the form $k^2\varepsilon_2(k)$ and $k^2\varepsilon_1(k)$ determine appearance of the first-order poles on the imaginary axis of the complex plane. The integrals are analytical everywhere, except these singular points. This allows one to substitute the integrals on the real axis K_Z by those in the corresponding contours on the complex plane and to integrate the integrals over the variable K_Z:

$$g_1(K,Z_0) = [\pi/(\varepsilon_p K)]\exp(-2KZ_0),$$

$$g_2(K,Z_0) = [\pi/(\varepsilon_p K)]\exp(-KZ_0),$$

$$g_3(K,Z_0) = g_2(K,Z_0),$$

$$g_4(K) = (\pi/K)\{1/\varepsilon_S + (1/\varepsilon* - 1/\varepsilon_S)/[1 + (KL)^{-2}]^{1/2}\}.$$

The following insertion of the calculated integrals to Eq. (A1) allows us to write $W(Z_0)$ as the integral function of variable K:

$$W(Z_0) = (Q^2/2\varepsilon_p)\int_0^{+\infty} dK\,\exp(-2KZ_0)\{1 - (2/\varepsilon_p)/F(K)\} \tag{A2}$$

where

$$F(K) = 1/\varepsilon_p + 1/\varepsilon_S + (1/\varepsilon* - 1/\varepsilon_S)/[1 + (KL)^{-2}]^{1/2}.$$

The simple transformation of the variable $(2KZ_0{=}x)$ in Eq. (A2) allows one to obtain the compact expression for $W(Z_0)$:

$$W(Z_0) = (Q^2/4\varepsilon_p Z_0)\int_0^{+\infty} dx S(x,\eta)\exp(-x), \tag{A3}$$

where

$$S(x,\eta) = [D(x,\eta) - 1/\varepsilon_p]/[D(x,\eta) + 1/\varepsilon_p],$$

$$D(x,\eta) = (1/\varepsilon_S) + (1/\varepsilon* - 1/\varepsilon_S)[1 + (x\eta)^{-2}]^{-1/2}$$

and

$$\eta = L/2Z_0.$$

[1] A. H. Elcock, D. Sept, and J. A. McCammon, J. Phys. Chem. B **105**, 1504 (2001).
[2] C. L. Vizcarra and S. L. Mayo, Curr. Opin. Chem. Biol. **9**, 622 (2005).
[3] P. Koehl, Curr. Opin. Struct. Biol. **16**, 142 (2006).
[4] R. M. Levy and E. Gallicchio, Annu. Rev. Phys. Chem. **49**, 531 (1998).
[5] C. J. Wilson, R. E. Clegg, D. I. Leavesley, and M. J. Pearcy, Tissue Eng. **11**, 1 (2005).
[6] J. J. Gray, Curr. Opin. Struct. Biol. **14**, 110 (2004).
[7] D. Asthagiri and A. M. Lenhoff, Langmuir **13**, 6761 (1997).
[8] K. Wilson, S. J. Stuart, A. Garcia, and R. A. Lator, Jr., J. Biomed. Mater. Res. **69A**, 686 (2004).
[9] F. Namavar, R. F. Sabirianov, A. I. Rubinstein, J. D. Jackson, J. G. Sharp, R. M. Namavar, H. Haider, E. V. Fehringer, and K. L. Garvin, in *Surface-Reactive Biomaterials as Scaffolds and Coatings: Interactions with Cells and Tissues*, edited by A. Ravaglioli, and A. Krajewski [National Research Council (CNR), Faenza, Italy, 2009], pp. 34–43.
[10] C. L. Cheung, A. I. Rubinstein, E. Peterson, A. Chatterji, R. F. Sabirianov, W.-N. Mei, T. Lin, J. E. Johnson, and J. J. DeYoreo, Langmuir **26**, 3498 (2010).
[11] F. B. Sheinerman, R. Norel, and B. Honig, Curr. Opin. Struct. Biol. **10**, 153 (2000).
[12] T. Shira, S. Albeck, and G. Schreiber, Nat. Struct. Biol. **7**, 537 (2000).
[13] D. Sept, A. H. Elcock, and J. A. McCammon, J. Mol. Biol. **294**, 1181 (1999).
[14] D. Xu, S. L. Lin, and R. Nussinov, J. Mol. Biol. **265**, 68 (1997).
[15] L. D. Drozdov-Tikhomirov, D. M. Linde, V. V. Poroikov, A. A. Alexandrov, and G. I. Skurida, J. Biomol. Struct. Dyn. **19**, 279 (2001).
[16] F. Glaser, D. M. Stainberg, I. A. Vakser, and N. Ben-Tal, Proteins **43**, 89 (2001).
[17] T. Wang, S. Tomic, R. R. Gabdoulline, and R. C. Wade, Biophys. J. **87**, 1618 (2004).
[18] L. D. Drozdov-Tikhomirov, D. M. Linde, V. V. Poroikov, A. A. Alexandrov, G. I. Skurida, P. V. Kovalev, and V. Yu. Potapov, J. Biomol. Struct. Dyn. **21**, 257 (2003).
[19] G. Schreiber and A. R. Fersht, Nat. Struct. Biol. **3**, 427 (1996).
[20] J. Janin, Proteins **28**, 153 (1997).
[21] M. Vijayakumar, K.-Y. Wung, G. Schreiber, A. R. Fersht, A. Szabo, and H.-X. Zhou, J. Mol. Biol. **278**, 1015 (1998).
[22] Y. Shaul and G. Schreiber, Proteins **60**, 341 (2005).
[23] A. J. McCoy, E. V. Chandana, and P. M. Colman, J. Mol. Biol. **268**, 570 (1997).
[24] V. A. Roberts, H. C. Freeman, A. J. Olson, J. A. Tainer, and E. D. Getzoff, J. Biol. Chem. **266**, 13431 (1991).
[25] H.-X. Zhou, Biopolymers **59**, 427 (2001).
[26] R. R. Gabdoulline and R. C. Wade, J. Mol. Biol. **306**, 1139 (2001).
[27] A. H. Elcock, R. R. Gabdoulline, R. C. Wade, and J. A. McCammon, J. Mol. Biol. **291**, 149 (1999).
[28] F. Dong, M. Vijayakumar, and H.-X. Zhou, Biophys. J. **85**, 49 (2003).
[29] F. Dong and H.-X. Zhou, Proteins **65**, 87 (2006).
[30] G. Schreiber and A. R. Fersht, J. Mol. Biol. **248**, 478 (1995).
[31] F. B. Sheinerman and B. Honig, J. Mol. Biol. **318**, 161 (2002).
[32] Z. S. Hendsch and B. Tidor, Protein Sci. **3**, 211 (1994).

[33] L.-P. Lee and B. Tidor, Protein Sci. **10**, 362 (2001).
[34] R. Luo, L. David, H. Hung, J. Devaney, and M. K. Gilson, J. Phys. Chem. B **103**, 727 (1999).
[35] M. K. Gilson, A. Rashin, R. Fine, and B. Honig, J. Mol. Biol. **184**, 503 (1985).
[36] A. Papazyan and A. Warshel, J. Phys. Chem. B **101**, 11254 (1997).
[37] J. D. Jackson, *Classical Electrodynamics* (Wiley, New York, 1998).
[38] A. Rubinstein and S. Sherman, Biophys. J. **87**, 1544 (2004).
[39] S. K. Pal, J. Peon, B. Bagchi, and A. H. Zewail, J. Phys. Chem. B **106**, 12376 (2002).
[40] S. K. Pal, J. Peon, and A. H. Zewail, Proc. Natl. Acad. Sci. U.S.A. **99**, 1763 (2002).
[41] S. K. Pal and A. H. Zewail, Chem. Rev. **104**, 2099 (2004).
[42] J. Higo and M. J. Nakasako, J. Comput. Chem. **23**, 1323 (2002).
[43] S. M. Bhattacharyya, Z.-G. Wang, and A. H. Zewail, J. Phys. Chem. B **107**, 13218 (2003).
[44] J. Higo, M. Sasal, H. Sasai, H. Nakamura, and T. Kugimiya, Proc. Natl. Acad. Sci. U.S.A. **98**, 5961 (2001).
[45] C. Rocchi, A. R. Bizzarri, and S. Cannistraro, Phys. Rev. E **57**, 3315 (1998).
[46] F. Massi and J. E. Straub, J. Comput. Chem. **24**, 143 (2003).
[47] A. Rubinstein and S. Sherman, Biopolymers **87**, 149 (2007).
[48] A. A. Kornyshev and M. A. Vorotyntsev, Surf. Sci. **101**, 23 (1980).
[49] A. I. Rubinshtein, Sov. Electrochem. **16**, 1436 (1981).
[50] A. A. Kornyshev, A. I. Rubinshtein, and M. A. Vorotyntsev, J. Phys. C **11**, 3307 (1978).
[51] A. I. Rubinshtein, Phys. Status Solidi B **120**, 65 (1983).
[52] V. K. Misra, J. L. Hecht, A. S. Yang, and B. Honig, Biophys. J. **75**, 2262 (1998).
[53] A. A. Kornyshev, Electrochim. Acta **26**, 1 (1981).
[54] A. A. Kornyshev and G. J. Sutmann, Chem. Phys. **104**, 1524 (1996).
[55] A. A. Kornyshev and J. Ulstrup, Chem. Phys. Lett. **126**, 74 (1986).
[56] A. A. Kornyshev, in *The Chemical Physics of Solvation*, edited by R. R. Dogonadze, E. Kalman, A. A. Kornyshev, and J. Ulstrup (Elsevier, Amsterdam, 1985), pp. 77–118.
[57] A. I. Rubinshtein, Sov. Electrochem. **21**, 433 (1985).
[58] O. I. Obolensky, T. P. Doerr, R. Ray, and Y.-K. Yu, Phys. Rev. E **79**, 041907 (2009).